A theoretical and experimental study of non-linear absorption properties of substituted 2,5-di-(phenylethynyl)thiophenes and structurally related compounds.

Per Lind, Marcus Carlsson, Bertil Eliasson, Eirik Glimsdal, Mikael Lindgren, Cesar Lopes, Linus Boman, Patrick Boman

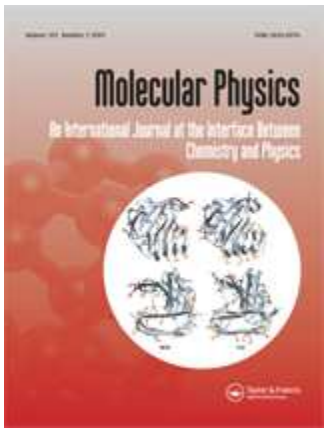

A theoretical and experimental study of non-linear absorption properties of substituted 2,5-di-(phenylethynyl)thiophenes and structurally related compounds.

Journal:	*Molecular Physics*
Manuscript ID:	TMPH-2008-0296.R1
Manuscript Type:	Full Paper
Date Submitted by the Author:	19-Feb-2009
Complete List of Authors:	Lind, Per; NBC Defence, FOI Carlsson, Marcus; Department of Chemistry Eliasson, Bertil; Department of Chemistry Glimsdal, Eirik; Department of Physics Lindgren, Mikael; Department of Physics Lopes, Cesar; Division of Sensor Technology Boman, Linus; Department of Physics, Chemistry and Biology Boman, Patrick; Department of Physics, Chemistry and Biology
Keywords:	Density functional theory, Two-photon absorption, Excited state absorption, Optical limiting, Chalcogenophenes

A theoretical and experimental study of non-linear absorption properties of substituted 2,5-di-(phenylethynyl)thiophenes and structurally related compounds

Per Lind [a,b], Marcus Carlsson [a], Bertil Eliasson [a,i] , Eirik Glimsdal [c], Mikael Lindgren [b,c], Cesar Lopes [d], Linus Boman [e], Patrick Norman [e,i]

[a] *Department of Chemistry, Umeå University, SE-901 87 Umeå, Sweden*

[b] *NBC Defence, FOI, Cementvägen 20, SE-901 82 Umeå, Sweden*

[c] *Department of Physics, Norwegian University of Science and Technology (NTNU), NO-7491 Trondheim, Norway*

[d] *Division of Sensor Technology, Swedish Defence Research Agency (FOI), SE-581 11 Linköping, Sweden*

[e] *Department of Physics, Chemistry and Biology, Linköping University, SE-581 83 Linköping, Sweden*

Keywords: Density functional theory, Two-photon absorption, Excited state absorption, Optical limiting, Chalcogenophenes, Thiophenes, DFT, TPA

Abstract

Photo-physical properties relevant for optical power limiting in the near-visible and visible regions of the spectrum are reported for a series of substituted diarylalkynyl chalcogenophenes (furans, thiophenes, selenophenes, and tellurophenes). The linear ground and excited state absorption as well as the nonlinear two-photon absorption were determined at the time-dependent density functional theory level with use of the hybrid exchange-correlation functionals B3LYP and CAM-B3LYP. A selected number of the theoretically studied molecules were synthesized and characterized experimentally with the use of absorption and luminescence spectroscopy. The photo-physical data are compared to the results from optical power limiting measurements performed in THF solution at a wavelength of 532 nm, with a laser pulse length of 5 ns and pulse energies

[i] Corresponding authors. E-mail address (Eliasson): bertil.eliasson@chem.umu.se, E-mail address (Norman): panor@ifm.liu.se.

up to 150 μJ. The best compounds in the present investigation display an energy damping of approximately a factor of 10 at a concentration of 0.010 M.

1. Introduction

The interest for third-order nonlinear optical (NLO) properties of organic materials has grown considerably during the last two decades due to the potential of finding inexpensive and easily processable materials for different optical applications including all-optical signal processing [1-7]. These applications can, for instance, take advantage of two-photon absorption/emission and third harmonic generation properties of the materials [7-9]. Our interest in this area involves nonlinear absorption as a means for protection of eyes and various types of sensors in optical equipment from laser beams operating at wavelengths in the visible region [6,10-12]. A primary requirement of the material is fast switching from high transparency for normal light (or low laser power) to non-transparency at high laser incident fluences. Such fast optical power limiting (OPL) may be obtained by the molecular process excited-state absorption (ESA), possibly in conjunction with two-photon absorption (TPA) which typically occurs only at high laser irradiance [6,7,10,13-15].

Many studies have shown that an extended molecular π-electron system is an important characteristic for achieving large NLO effects [7,16-18]. Among the large number of molecules, oligomers and polymers that have been investigated for NLO properties, it is common that benzenoid rings are present in the structures. Often, the aromatic rings are linked together via acetylene groups, and this appears to be a useful element in the design of NLO systems [16,19].

In earlier work on relatively small molecules with benzenoid rings and heteroatom-containing aromatic rings, we performed measurements of OPL at 532 nm [20-22]. It was found that 2,5-di(phenylethynyl) thiophenes and a corresponding furan gave interesting results. Moreover, such structures can easily be synthesized and their π-systems can be widely modified and extended by standard coupling reactions. Even though significantly better OPL properties were reported from studies of e.g. phthalocyanines and diarylalkynyl-bisphosphine Pt(II) complexes [12,23,24], thiophene compounds have other beneficial properties. The transparency in the visible range and

the solubility are generally high, and high-concentration samples may thus compensate for the lower OPL effect per molecule of the thiophenes.

Here, we present the continuation of our studies on the thiophene derivatives to gain more insight into the mechanisms responsible for OPL in these systems. Experimental time- and spectrally-resolved luminescence data of a series of new compounds are interpreted with the aid of results from quantum chemistry modeling of both one- and two-photon excitations. Thus, on the basis of density functional theory (DFT) we discuss ESA and TPA with respect to the lowest excited singlet state as the origin for OPL at 532 nm for ns pulses. The structures of the thiophenes and the other chalcogenophenes in this study are shown in Figure 1.

Figure 1 can be inserted here

2. Experimental and computational details

2.1. Quantum chemical calculations

Structure optimizations of all molecules were performed with the Gaussian 03 program [25], at the DFT level of theory using the hybrid B3LYP [26] exchange-correlation functional and Dunning's correlation consistent cc-pVDZ basis set [27] for the H, C, N and O atoms and the Stuttgart effective core potentials (ECPs) [28] for S, Se and Te (using valence basis sets with polarizing *d*-functions). All molecular structures were optimized in the C_{2v} point group, with the *z*-axis being the principle axis and the *y*-axis being the conjugation axis. The three components of the electric-dipole operator (μ_x, μ_y, and μ_z) thereby span the irreducible representations B_1, B_2, and A_1, respectively.
The molecular property calculations were carried out with the Dalton program [29] at the time-dependent Hartree-Fock and DFT levels of theory. In addition to the use of the B3LYP functional we have also employed the Coulomb attenuated B3LYP (CAM-B3LYP) [30] functional in order to obtain a correct asymptotic Coulomb interaction between the hole and electron orbitals in the excitation processes. This version of the Dalton program includes an implementation of the CAM-B3LYP functional by Peach *et al*. [31].

The all-electron basis sets used in the property calculations are based on the standard 6-31G basis set [32] and the cc-pVDZ and cc-pVTZ basis sets of Dunning [27], but additional diffuse and polarization functions have been added as stated in the text and tables.

The one-photon transition moments describing the ground state linear absorption were obtained from the first-order residue of the electric-dipole polarizability, whereas those describing excited state absorption were obtained from the second-order residue of the first-order hyperpolarizability. The two-photon transition moments were identified from the first-order residue of the hyperpolarizability. A detailed presentation of the relations between linear and nonlinear response functions and the one- and two-photon transition moments is found in the work of Norman and Ruud [33]. The equations are also summarized in a contribution by Samoc et al. [34]. For linear as well as nonlinear absorption the corresponding absorption cross sections are proportional to the squares of the respective moments. In one-photon absorption processes it is customary to give the dimensionless oscillator strength (*f*) as the measure of absorption strength and we adopt to this tradition, and for the two-photon absorption process we present cross sections (σ^{TP}) in units of Göppert-Mayer (GM).

2.2. Measurements and instrumentation

IR spectra were recorded for neat compounds using a Mattson ATI 60AR FTIR equipped with a Golden Gate Single Reflection Diamond ATR accessory. ^{1}H and ^{13}C NMR measurements were carried out on a Bruker DRX 400 MHz, and chemical shifts are reported relative to TMS as internal reference using $CDCl_3$ as solvent. Mass spectra were obtained from a JMS-SX/SX102A double focusing magnetic sector mass spectrometer (Jeol, Tokyo), using direct inlet and electron impact ionisation (EI+), with ionizing voltage 70 eV, acceleration voltage 10 kV, and resolution 1000. Elemental analyses were performed by Mikrokemi AB, Uppsala, Sweden. Optical limiting spectra were recorded with a f/5 focusing system using a frequency doubled Nd:YAG laser delivering 5 ns pulses at 532 nm with a repetition rate of 10 Hz [35,36]. OPL data were obtained for tetrahydrofuran (THF) solutions in 2 mm quartz cuvets. THF of p.a. quality was used for photophysical measurements. The OPL of neat THF in a quartz cuvet was found to be insignificant compared with that of solutions of the investigated compounds. UV-visible spectra were recorded on a Shimadzu UV-3101PC spectrophotometer in dual mode using 10 mm quartz cells and THF as solvent and were

repeated on a Shimadzu UV-1601PC spectrometer for the fluorescence quantum yield measurements. A mode locked Titanium:Sapphire laser (Coherent Mira 900-F) was used as excitation source for the luminescence measurements. For the steady-state luminescence and time-resolved measurements at 350-360 nm, the fundamental laser beam at wavelength 700-720 nm was frequency doubled using a SHG crystal (Inrad Ultrafast Harmonic Generation System, Model 5-050). For the corresponding measurements at 337 nm, a diode laser was used. The emission spectra and emission decay traces were taken on a Jobin Yvon IBH FluoroCube spectrometer using the Time-Correlated Single-Photon Counting (TCSPC) mode. IBH DataStation v 2.1 software was used for operation of the spectrometer. The fluorescence quantum yields were determined relative to the quantum yields of a reference system of Coumarin 110 (0.62) [37]. The data were analyzed according to a procedure reported by Williams et al. [38].

2.3. Synthesis

Phenylacetylene, 4-pentylphenylacetylene, 2,5-diiodothiophene, 2,3,5-tribromothiophene, triphenylphosphine (PPh_3), CuI and $PdCl_2(PPh_3)_2$ were obtained from Aldrich and were used as received. Triethylamine (TEA), pyridine and the solvents used in the reactions were of p.a. quality. TLC was performed on silica gel 60 F_{254} (Merck) and flash column chromatography was performed on silia gel (Matrex 60 Å, 35-70 μm, Grace Amicon). 2,5-Di(4-pentylphenylethynyl)thiophene (**S1-Pe**), 3-dodecyl-2,5-di(4-(4-pentylphenylethynyl)phenylethynyl)thiophene (**S2-Pe**), and 3-dodecyl-2,5-di(4-(4-(4-pentylphenylethynyl)phenylethynyl)phenylethynyl)thiophene (**S3-Pe**), were prepared as previously reported [21]. The last step in the synthesis of the target compounds was a Pd(0)-Cu(I)-catalyzed cross-coupling (Scheme) [39]. Even though a comparison with a tellurophene such as **Te1** or **Te1-Pe** was planned, attempts to synthesize tellurophenes indicated that their thermal stability would not be sufficient for OPL experiments, and the work was therefore suspended.

Scheme can be inserted here

2.3.1. 2,5-Di(4-pentylphenylethynyl)furan (**O1-Pe**)

2,5-Dibromofuran [40] (0.43 g, 1.9 mmol) was dissolved in a mixture of 20 ml tetrahydrofuran (THF) and 15 ml TEA under argon atmosphere. To the solution was

added CuI (25 mg, 0.13 mmol), $PdCl_2(PPh_3)_2$ (60 mg, 0.085 mmol) followed by dropwise addition of the alkyne (1.0 g, 5.8 mmol). The color of the solution changed rapidly from orange to pale yellow. The reaction mixture was heated to reflux and stirred for 20 h. The solvent was removed under reduced pressure and the residue was dissolved in CH_2Cl_2, washed with 50 ml 1 M HCl and water. The organic phase was dried with $MgSO_4$, concentrated and flash chromatographed on silica using heptane as eluent. The product was obtained as white crystals, 0.36 g (46 %). IR: $\nu(cm^{-1})$ 2207; ^{1}H-NMR ($CDCl_3$): δ 7.42 (d, J = 8 Hz, 4H), 7.15 (d, J = 8 Hz, 4H), 6.61 (s, 2H), 2.59 (t, J = 8 Hz, 4H), 1.59 (m, 4H), 1.29 (m, 8H), 0.87 (t, J = 7 Hz, 6H); ^{13}C-NMR ($CDCl_3$): δ 144.2; 137.7, 131.4, 128.5, 119.1, 115.9, 94.3, 78.7, 35.9, 31.4, 30.9, 22.5, 14.0; EI+ MS: m/z (int %) 84 (100), 408 (55); Anal. Calcd. for $C_{30}H_{32}O$ (%): C, 88.19; H, 7.89; Found: C, 88.3; H, 8.0.

2.3.2. 2,5-Di(phenylethynyl)thiophene (**S1**)

This compound was synthesized similar to a known procedure [41], but using 2,5-diiodothiophene, TEA and $PdCl_2(PPh_3)_2$ instead of the reported chemicals. The workup and chromatography were done as described for **O1-Pe**. The product was obtained in 74 % yield. The IR and NMR (^{1}H, ^{13}C) data were in accord with those reported in ref. [41].

2.3.3. 2,5-Di-(4-methoxyphenylethynyl)thiophene (**S1-OMe**)

The reaction was performed in a Smith Synthesizer single-mode microwave cavity (Personal Chemistry AB, Uppsala, Sweden). To a heavy-walled glass Smith process vial, 2,5-diiodothiophene (0.20 g, 0.60 mmol), CuI (40 mg, 0.21 mmol), PPh_3 (50 mg, 0.19 mmol), $PdCl_2(PPh_3)_2$ (92 mg, 0.13 mmol), 1-ethynyl-4-methoxy-benzene (0.20 g, 1.5 mmol), dimethylformamide (1.5 ml) and TEA (1.5 ml) was added. A small magnet was used for stirring and the vial was sealed with an aluminium crimp cap fitted with a silicon septum. The reaction was performed at 120 °C for 240 s. The workup and chromatography (heptane/ethyl acetate 20:1) were done as described for **O1-Pe**. A yellow solid (0.17 g, 83 % yield) was obtained. IR: $\nu(cm^{-1})$ 2202; ^{1}H NMR (400 MHz, $CDCl_3$): δ 7.46 (d, J = 9 Hz, 4H), 7.11 (s, 2H), 6.88 (d, J = 9 Hz, 4H), 3.83 (s, 6H); ^{13}C NMR (100 MHz, $CDCl_3$): δ 160.02, 133.11, 131.44, 124.7, 114.8, 114.18, 94.06, 81.21, 55.41; Anal. Calcd. for $C_{22}H_{16}O_2S$ (%): C, 76.72; H, 4.68; Found: C, 76.7; H, 4.8.

2.3.4. 2,5-Di(4-pentylphenylethynyl)-3,4-dinitrothiophene (**S1-NO2-Pe**)

2,5-Dibromo-3,4-dinitrothiophene (0.50 g, 1.5 mmol) was dissolved in a mixture of 10 ml THF and 10 ml TEA under argon atmosphere. To the solution was added CuI (20 mg, 0.11 mmol), $PdCl_2(PPh_3)_2$ (40 mg, 0.057 mmol) and PPh_3 (30 mg, 0.12 mmol), followed by dropwise addition of the alkyne (0.80 g, 4.6 mmol). The color of the solution changed rapidly from pale yellow to red. The reaction mixture was stirred for 20 h at room temperature and was refluxed for an additional 4 h. The workup and chromatography were done as described for **O1-Pe**. After recrystallization from hexane the product was obtained as orange crystals, 100 mg (13 %). IR: $\nu(cm^{-1})$ 2202; ^{1}H-NMR ($CDCl_3$): δ 7.47 (d, J = 8 Hz, 4H), 7.20 (d, J = 8 Hz, 4H), 2.61 (t, J = 8 Hz, 4H), 1.61 (m, 4H), 1.31 (m, 8H), 0.89 (t, J = 7 Hz, 6H); ^{13}C-NMR ($CDCl_3$): δ 147.2, 141.0, 133.0, 129.6, 123.3, 118.2, 106.6, 77.4, 36.8, 32.1, 31.5, 23.2, 14.7. Anal. Calcd. for $C_{30}H_{30}N_2O_4S$ (%): C, 70.01; H, 5.88; Found: C, 70.1; H, 6.0.

2.3.5. 2,3,5-Tri(4-pentylphenylethynyl)thiophene (**S1A-Pe**)

2,3,5-Tribromothiophene (1.9 g, 5.9 mmol) was dissolved in a deoxygenated mixture of 20 ml dry pyridine and 20 ml dry TEA under argon atmosphere. $PdCl_2(PPh_3)_2$ (0.10 g, 0.14 mmol), and CuI (0.1 g, 0.05 mmol) were added to the solution, followed by dropwise addition of 4-pentyl-1-ethynylbenzene (4.0 g, 23 mmol). The reaction was stirred for 24 hours at room temperature followed by reflux for an additional 48 hours. A dark solution was formed. The workup and chromatography were done as described for **O1-Pe**. A red oil was obtained, 0.98 g (27 %). IR: $\nu(cm^{-1})$ 2195; ^{1}H NMR ($CDCl_3$): δ 7.46 (d, J = 8 Hz, 4H), 7.40 (d, J = 8 Hz, 2H), 7.19 (s, 1H), 7.15 (m, 6H), 2.61 (t, J = 8 Hz, 6H), 1.61 (m, 6H), 1.31 (m, 12H), 0.89 (t, J = 7 Hz, 9H); ^{13}C NMR ($CDCl_3$): δ 144.1, 144.1, 143.7, 133.3, 131.6, 131.5, 128.5, 128.5, 126.7, 126.5, 123.3, 120.1, 119.8, 119.5, 98.6, 94.6, 93.7, 82.9, 81.4, 81.2, 35.9, 31.4, 30.9, 30.9, 22.5, 14.0; EI+ MS: m/z (int %) = 424 (100), 594 (0.3). Anal. Calcd. for $C_{43}H_{46}S$ (%): C, 86.82; H, 7.79; Found: C, 86.5; H, 8.1.

2.3.6. 2,5-Di(phenylethynyl)selenophene (**Se1**)

2,5-Dibromoselenophene [42] (0.069 g, 0.24 mmol) was dissolved in a mixture of THF (1.5 ml) and TEA (1.5 ml) under Ar atmosphere. $PdCl_2(PPh_3)_2$ (5 mg, 0.007 mmol), CuI (2 mg, 0.01 mmol) and PPh_3 (2.0 mg, 0.008 mmol) was added to the solution, followed

by dropwise addition of phenylacetylene (0.026 g , 0.25 mmol). The reaction was stirred for 48 h at room temperature. The workup and chromatography were done as described for **O1-Pe**. The product was obtained as a yellow white solid, 0.039 g, in 49 % yield; IR: $\nu(cm^{-1})$: 2198 s; ^{1}H-NMR ($CDCl_3$): δ 7.55-7.49 (m, 4H), 7.38-7.31 (m, 8 H); ^{13}C-NMR ($CDCl_3$): δ 134.27, 131.48, 129.44, 128.73, 128.52, 122.89, 96.07, 84.72. Anal. Calcd. for C20H12Se (%): C, 72.51; H, 3.65; Found: C, 72.2; H, 3.8.

3. Results and discussion

In order to have ESA to function well for OPL, the absorption coefficient for transition from the electronic ground state (S_0) to an excited state should be relatively small to provide the high transmittance at normal light intensity, but should be non-zero so that the excited state nevertheless can become populated by high-intensity light. In addition, the absorption from the initial excited state to higher electronic states should be large. Relaxation from the upper excited states should be fast enough to avoid depletion of the levels associated with the important absorption processes. Intersystem crossing from excited singlet to triplet (T) states having strong optical absorption can be advantageous since T states generally have longer lifetimes than excited singlet states.

To aid in the design of OPL chromophores, one-photon absorption (OPA), ESA and TPA properties were calculated for compounds previously prepared in our laboratory or for model compounds of these, and for a few structurally related compounds not prepared earlier. Several of the synthesized compounds had alkyl substituents to improve solubility. To shorten the time for the quantum chemistry calculations, the alkyl groups were replaced by hydrogens. Two new compounds were subsequently synthesized and their OPL were measured at the wavelength of 532 nm, for the comparison with calculated data. As stated in the Experimental section, geometry optimizations were performed using the B3LYP method with cc-pVDZ and ECP basis sets. For all compounds, the outer rings were found to be coplanar with the central ring, but since the barrier for interring twisting is expected to be low [43], the experimental data will likely represent an average of conformations with varying degree of interring twist. Because of this, we will limit our comparisons to calculated excitation energies and peak maxima in the experimental absorption spectra, and generally not

discuss band shapes. From a recently reported single-crystal structure of **S1**, as determined by X-ray diffraction at 120 K [44], we could compare some bond lengths of that structure with our optimized geometry of **S1**. We found that the two structures have bond lengths that agree within 0.2-2.1 pm for the central ring bonds and the $C_{2,5}$-C(triple), and CC(triple) bonds. Hence, we do not expect errors in geometrical parameters to significantly contribute to differences between theoretical and experimental excitation energies.

In the following sections, results from the theoretical work are presented first, followed by the results of experimental absorption and fluorescence data.

3.1. Calculations of one-photon absorption

The calculations of electronic absorption spectra were performed using first-principles methods. The core electron densities of S, Se and Te were not included explicitly in the parameterization of the Hartree-Fock and Kohn-Sham determinants, but, instead, relativistic spin-free ECPs were used. This approach does not only reduce the computational effort but also increase the accuracy by providing relativistically correct potentials for the motions of the valence electrons. We have previously made a series of benchmarking calculations that show the virtues and limitations of ECP calculations for linear and nonlinear valence electron properties [34,45-47]. In summary, these investigations showed that excitation energies and one-photon moments can be quite accurately determined with use of ECPs but that two-photon moments in reality break spin selection rules even for light compounds. (The integrated TPA cross sections may, however, be of fair quality with the ECP approach) [46].

The electronic structure of the ground state of all molecules in the present study is closed-shell in nature and the ground state is therefore denoted as X^1A_1 in all cases. The one-photon absorption spectra will be dominated by spin-allowed transitions to states of spatial B_2 symmetry, i.e., transitions induced by an electric field polarized along the molecular conjugation axis. The lowest transition of this type is well characterized by an electronic transition from the highest-occupied molecular orbital (HOMO) to the lowest-unoccupied molecular orbital (LUMO). Both these MOs are of π-type and the HOMO (of symmetry A_2) has a node in the *xz*-plane while the LUMO (of symmetry B_1) has a significant electron density at the position of the heavy atom.

An investigation of the sensitivity of the linear absorption spectra with respect to computational parameters was performed for compound **S1** and the results from this

investigation are compiled in Table 1. From the results presented in the table it can be concluded that the use of ECPs (which in a sense corresponds to a frozen core electron density) does not inflict a loss in accuracy for linear absorption properties; if one compares the two first rows, it is seen that the excitation wavelength (λ_{exc}) and the oscillator strength is practically unchanged from the all-electron calculation to the corresponding ECP calculation. This justifies the use of the ECPs for the heavy atoms in the remainder of this work. It can also be concluded from the B3LYP and B3LYP-CAM results in Table 1 that the double-ζ basis set [cc-pVDZ+ECP(pd)] is sufficient in order to describe this valence electron transition (the excitation wavelength differs no more than 4 nm when compared to the result obtained with the corresponding triple-ζ basis set). The experimental absorption maximum (λ_{max}) is found at a wavelength of 348 nm for **S1** in THF, see Table 2. One explanation for the smaller value of λ_{max} compared to the CAM-B3LYP/daug-cc-pVDZ value of 363 nm can be that conformations with an inter-ring twist, and hence lower conjugation, contribute to the former value. In the present work, we have chosen not to address solvent effects and nuclear vibrations, and will thus accept discrepancies of this size between theoretical and experimental results.

Recent developments of exchange-correlation functionals have shown that such functionals based on the Coulomb attenuated method give an appropriate description of time-dependent response properties. For instance, it has been found that the CAM-B3LYP functional performs well for estimations of excitation energies of organic dyes [48,49], and can give results in close agreement with coupled cluster methods for calculations of TPA energies and transition strengths of valence excited states [50]. We therefore consider the CAM-B3LYP results of linear as well as nonlinear response properties to be the most appropriate in this study. Concerning the various choices of basis sets that appear in Table 1, we consider the best to be the cc-pVDZ basis set augmented with two sets of diffuse functions (daug-cc-pVDZ). However, from the results in the table it is clear that single augmentation is adequate in the present case, and in the discussion below the CAM-B3LYP/aug-cc-pVDZ results are considered to be the theoretical reference data.

Table 1 can be inserted here

The linear absorption of several other chalcogenophenes was calculated and the results are presented in Table 2. Notice that many of the molecular structures for

calculations were simplified in order to reduce the computational efforts, but that the calculated and experimental data are comparable for structures which differ only by the length of the alkyl chain or where the alkyl chain is 'replaced' with a hydrogen, since such modifications should have only small effects on the π-system of the compound. A comparison between the calculated data shows the same trends as discussed above with respect to method and basis set. It is also found that although the choice of method and to some degree basis set has an effect on the absolute values of excitation wavelengths and oscillator strengths, the relative order amongst the molecules remains the same. The dominating linear absorption for the compounds with short conjugation length is generally found in the ultraviolet region just outside the visible range, and the compounds were thus expected to be only slightly coloured. A red-shift in the absorption occurs when: (a) the number of repeat units in the ligands is increased, which results in an increased charge-conjugation length and a smaller bandgap, or (b) the heteroatom in the ring is replaced by a heavier atom, which can be explained by the smaller energy gap between occupied and virtual orbitals in heavy atoms. The comparison of the experimental values for **S1** and **S1-Pe** shows that the substitution of the peripheral alkyl group for hydrogen only slightly changes the value of λ_{max}. With the reasonable assumption that this is valid also for comparisons of **O1-Me** and **O1-Pe** with the alkyl- or unsubstituted S, Se and Te compounds, it is noticed that the CAM-B3LYP calculated redshift of 13 nm from **O1-Me** to **S1** is in good agreement with the λ_{max} redshifts from **O1-Pe** to **S1** and **O1-Pe** to **S1-Pe** of 10 nm and 14 nm, respectively. The absorption redshift as due to a substitution of selenium for sulfur (**Se1** compared to **S1**) is 14 nm at the CAM-B3LYP level of theory and 11 nm in the experiment. The redshift as due to a substitution of tellurium for selenium (**Te1** compared to **Se1**) is predicted to be 13 nm at the same level of theory. We have not been able to synthesize the tellurophene compounds and can therefore not make a comparison with experiment in this case.

The presence of the OCH_3 termination group instead of H for the S, Se and Te compounds does not affect the theoretical band-gap energies significantly. On the other hand, the dipole moments are largely affected and this could be expected to have an effect on the solvent organization in ground and excited states. However, the difference in λ_{max} between **S1** and **S1-OMe** (8 nm) is virtually the same as the CAM-B3LYP value (6 nm). Further, we found that λ_{max} of **S1-OMe** differs very little between THF (356

nm) and toluene (358 nm) solution, which suggests that THF can be regarded as a nonpolar solvent in the context of excitations in the compounds of this study.

For **S1-NO2a** as compared to **S1**, a red-shift of 27 nm is predicted at the CAM-B3LYP level. Because such a shift will result in more coloured samples, the alternative structure **S1-NO2b**, with the nitro groups in positions 3 and 4 in the ring, was also examined theoretically. In this configuration, with adjacent NO_2 groups, the N and O atoms cannot be coplanar with the ring atoms due to steric reasons [51]. A twist of the NO_2 groups relative to the ring plane was also found by the calculations. The calculated excitation wavelength of **S1-NO2b** is quite similar to that of **S1**. Because of this expected favourable transmittance, **S1-NO2-Pe** instead of **S1-NO2a** was synthesized and characterized. It is clear from the results in Table 2, however, that the experimental redshift associated with the substitution of nitro groups for hydrogens amounts to 38 nm (λ_{max} of **S1-Pe** and **S1-NO2-Pe**), as compared to the blueshift of 2 nm in theory. Such a large quantitative and also qualitative discrepancy in results may be due to solvation effects associated with the large changes in dipole moment on excitation.

Table 2 can be inserted here

In concern with the theoretical calculations of the linear absorption spectra of the chalcogenophenes we conclude that the Coulomb attenuated functional is needed for an appropriate description of the dominating electronic transitions of the compounds. With use of the CAM-B3LYP functional, we obtain a realistic description of the unsubstituted, alkyl- and methoxy-substituted chalcogenophene compounds, where calculated transition wavelengths and heavy-atom induced redshifts agree well with experiment. However, for compounds with nitro groups, we suspect that solvation effects associated with large dipole moment changes can influence the data, which we have not accounted for.

In the presentation below of excited state and nonlinear absorption properties, we will restrict ourselves to only provide results obtained with the CAM-B3LYP functional.

3.2. Calculations of excited state absorption

The dominating state in the linear absorption spectrum is 1^1B_2 in all systems included in the present study, and we have therefore focused calculations of excited state absorption

to a situation where this state is the initial state in the absorption process. The final state is of singlet spin symmetry and, due to the predominance for absorption of light polarized along the conjugation axis, the spatial symmetry will be A_1. ESA calculations were performed on unsubstituted, methoxy- and nitro-substituted compounds, see Table 3. As a general trend, the CAM-B3LYP results suggest strong ESA in the red end of the visible region for all compounds. It is also noted that the wavelength of the transition with largest oscillation strength is shifted towards lower values in the order **O1-Me**, **S1**, **Se1**, **Te1** (807, 788, 748 and 735 nm, respectively). The same trend is found for the three methoxy-substituted compounds (806, 737 and 725 nm, respectively). We note that the ESA of **S1** has also been determined using the double augmented basis set (see footnote "a" of Table 3) and that the results for the dominant transitions are in close agreement with the results obtained using the single augmented basis set. However, an electronic transition appears at 415 nm at the CAM-B3LYP/daug-cc-pVDZ level with an oscillator strength of 0.093, which may contribute to the OPL in the blue region. The theoretical results indicate that there is much to gain in the OPL performance in the blue and green regions of the spectrum by enhancing the singlet state ESA in those regions. The blueshifts associated with the heavy-atom substitutions are not sufficient in this respect.

Table 3 can be inserted here

3.3. Calculations of two-photon absorption

In the present systems, the absorption of two photons in a simultaneous coherent process is only effective if both light quanta are polarized along the conjugation axis and the final state in the process is therefore of A_1 symmetry. The dominating states in the TPA spectra of the studied molecules are those that we have discussed in concern with excited state absorption. In Figure 2, we have plotted the TPA cross section values above 1 GM for the wavelength region of 400-650 nm, as obtained at the CAM-B3LYP/aug-cc-pVDZ level of theory. A TPA calculation was also performed with the daug-cc-pVDZ basis set for **S1**. This comparison between the single and double augmented basis sets show virtually unchanged absorption characteristics, with the two dominant TPA wavelengths above 400 nm found at 480 nm (σ^{TP} = 124 GM) and 497 nm (σ^{TP} = 193 GM) for both calculations.

The most striking observation to be made is that the TPA cross section does not strongly depend on heavy atom substitution. Compounds **O1-Me**, **S1**, **Se1** and **Te1** all have their largest absorption peak in the range of 487-508 nm, although additional somewhat weaker absorptions are found for **O1-Me** and **S1** at 413 and 480 nm, respectively. For **S1**, it is relevant to sum the intensities of the peaks at 480 and 495 nm; the total TPA cross section for these two states becomes about 330 GM which is close to the cross sections of **Se1** (350 GM) and **Te1** (360 GM). Hence, from a two-photon efficiency point of view the materials are quite identical but the absorption in **S1** is predicted to be somewhat broader than that of the other two due to the split of the intensity over two near-lying electronic states. In resemblance with these four compounds, the three methoxy-substituted compounds and **S1-NO2b** have their strongest TP absorptions close to 500 nm. All four of the latter compounds have additional noteworthy absorptions in the region of approximately 470-550 nm, but on the whole, the eight investigated compounds have rather similar TPA characteristics. (Although **Se1-OMe** has a strong TPA peak at 403 nm, this is not likely to be important since one-photon absorption can be expected to dominate at that wavelength).

With respect to the OPL characteristics of these compounds, the TPA bands around 500 nm are likely to contribute to absorption of 532 nm laser light due to the effects of vibrational broadening. The extent of its contribution (in comparison to ESA) is very difficult to predict without performing simulations of laser pulse propagation with account made for pulse shape, intensity, duration, etc. Such simulations are beyond the scope of the present work but have been initiated in our group on platinum-based compounds with focus on the contribution from the long-lived excited triplet states [52,53].

Figure 2 can be inserted here

3.4. UV-Visible absorption, OPL and steady state and time-resolved luminescence

The absorption spectra of the compounds in the wavelength range of 250-500 nm are dominated by one strong transition, with a vibrational substructure indicated (Figure 3). Certain compounds, such as **S2-Pe**, **S3-Pe** and notably **S1-NO2-Pe** and **S1A-Pe** appear to have at least two partially overlapping absorption bands, corresponding to

Figure 3 can be inserted here

different electronic states. The spectra of **S1** (not shown), **S1-Pe**, **S2-Pe**, **S3-Pe**, **S1-OMe** and **Se1** have very similar band shape (of the low-energy band) although the longer compounds have their bands red-shifted. The multi-component spectra of **S1A-Pe** and **S1-NO2-Pe** differ significantly from those of the other compounds by having a very broad and featureless band shape.

Optical limiting data are summarized in Table 4, as transmitted energy for each compound at a laser input energy of 150 μJ at 532 nm, for 5 ns pulses. It should be stressed that this comparison of compounds at a single wavelength is relevant for only a rather narrow wavelength region close to 532 nm. Some trends that can be found in the OPL results are: (a) the change of heteroatom in the ring from O to S results in a slightly inferior OPL result, but the change from S to Se improves the OPL capacity to the same level as for the corresponding furane; (b) the lengthening of the π-system provides better OPL in the order **S1-Pe** < **S2-Pe** < **S3-Pe**; [21] (c) with regard to the substitution pattern, the third phenylethynyl group in **S1A-Pe**, the methoxy groups in **S1-OMe**, and in particular the nitro groups in **S1-NO2-Pe**, result in better OPL for these compounds compared to that of **S1-Pe**.

Table 4 can be inserted here

In resemblance with absorption spectra, fluorescence of the compounds revealed peaks with vibrational substructure, however better resolved (Figure 4). The fluorescence quantum yields (Q_{fl}) and the lifetimes (τ_{fl}) increase in the order **S1-Pe** < **S2-Pe** < **S3-Pe** as do the OPL capacity at 532 nm, which might be expected if ESA contributes to the OPL process. The values of Q_{fl} and τ_{fl} are almost the same for **S1-OMe** and **S1-Pe**, and the somewhat lower OPL value of the former may well be explained by more efficient TPA due to the laser wavelength being slightly more appropriate for TPA in **S1-OMe**, see Figure 2. Both **S1-NO2-Pe** and **Se1** have very small values of Q_{fl} and τ_{fl}, and the better OPL of these compounds (particularly of the former) in comparison with **S1-Pe** is not easily explained by ESA from the 1^1B_2 state or

by TPA according to the results from the calculations. This shows that additional processes need to be considered. In the case of **Se1**, fast intersystem crossing from an excited singlet to the triplet state manifold due to the heavy-atom effect, with subsequent triplet state absorption, may contribute to the nonlinear absorption. Studies of organoselenium compounds have shown that intersystem crossing can compete with singlet internal conversion, although the latter process may be more efficient [54], and that degassed samples of Se tetramethylrosamine dyes can have a triplet quantum yield close to unity [55].

In the case of **S1-NO2-Pe**, the linear absorption band has a tail that extends into the green region (532 nm), which probably results in greater initial population of excited singlet states in comparison with other compounds in this study. As for **Se1**, the nonlinear absorption of **S1-NO2-Pe** may to some extent be explained by triplet formation and absorption within the triplet manifold. It is well known that aromatic nitro compounds, including 3,4-dinitrotoluene which has the nitro groups on adjacent carbons [56], can have fast singlet-to-triplet formation and high triplet quantum yields [56-58].

Figure 4 can be inserted here

The magnitude of the Stokes shifts, estimated from the lowest-energy peaks in the absorption and emission spectra, do not imply changes in the molecular conformations or solvent reorganization, with the exception of **S1-NO2-Pe** in chloroform (Table 4). In this compound, the HOMO-LUMO type of transition is associated with electron redistribution from the phenyl rings to the S atom and the NO_2 groups at the central ring, as found by the MO calculations. The Stokes shift can therefore, at least partly, be explained by a solvent redistribution after excitation. A twist of the nitro groups to increase conjugation in the excited state may also explain the Stokes shift. However, further studies are required to resolve this and the question regarding changes in molecular geometry in the excited state, as well as the dynamics and absorptions of **S1-NO2-Pe** in the excited state.

4. Summary

Time-dependent Hartree-Fock and DFT calculations of one-photon absorptions showed a good prediction of experimental wavelengths and oscillator strengths for the investigated chalcogenophenes. Calculations of two-photon absorptions indicated that several of the compounds should have a two-photon cross section of the same order of magnitude in a wavelength range of approximately 490-510 nm. At the wavelength for OPL measurements of the chalcogenophenes (532 nm) the TPA process can be expected to contribute significantly less to optical power limiting of these compounds. Absorption of the 1^1B_2 (excited singlet) state was calculated for several compounds at the CAM-B3LYP/aug-cc-pVDZ level, and the results showed significant ESA at the red end of the visible region, but virtually no absorption close to 532 nm.

The thiophene with nitro groups on the ring carbons (**S1-NO2-Pe**) showed the strongest OPL of the investigated compounds. The reason for this is not revealed by the calculations or the absorption/emission experiments, but greater initial population of the lowest excited state, in comparison with the other compounds, due to tailing of its absorption band into the green region (532 nm) may be part of the explanation.

Acknowledgements

This work was supported (BE, CL, ML, PN) by a Swedish Defence Nanotechnology Programme run jointly by the Swedish Defence Research Agency (FOI) and Defence Material Administration (FMV). ML acknowledges a grant from The Research Council of Norway within the NanoMat program, contract #163529.

References

[1] P.N. Prasad, B.A. Reinhardt, Chem. Mater. **2**, 660 (1990).
[2] J.L. Bredas, C. Adant, P. Tackx, A. Persoons, and B.M. Pierce, Chem. Rev. **94**, 243 (1994).
[3] G.I. Stegeman, Nonlinear Opt. Org. Mol. Polym., edited by H.S. Nalwa, S. Miyata (CRC Press, Boca Raton, 1997), p. 799.
[4] R.C. Hollins, Curr. Opi. Solid State Mat. Sci. **4**, 189 (1999).
[5] T. Kaino, J. Opt. A, Pure Appl. Opt. **2**, R1 (2000).
[6] G.J. Zhou, W.Y. Wong, C. Ye, and Z.Y. Lin, Adv. Funct. Mater. **17**, 963 (2007).
[7] G.S. He, L.-S. Tan, Q. Zheng, and P.N. Prasad, Chem. Rev. **108**, 1245 (2008).
[8] G. Ramos-Ortiz, M. Cha, S. Thayumanavan, J. Mendez, S.R. Marder, and B. Kippelen, Appl. Phys. Lett. **85**, 3348 (2004).
[9] K.S. Lee, D.Y. Yang, S.H. Park, and R.H. Kim, Polym. Adv. Technol. **17**, 72 (2006).
[10] J.W. Perry, Nonlinear Opt. Org. Mol. Polym., edited by H.S. Nalwa, S. Miyata (CRC Press, Boca Raton, 1997), p. 813.
[11] C.W. Spangler, J. Mater. Chem. **9**, 2013 (1999).
[12] D. Dini, M. Barthel, and M. Hanack, Eur. J. Org. Chem., 3759 (2001).
[13] J.E. Ehrlich, X.L. Wu, I.Y.S. Lee, Z.Y. Hu, H. Rockel, S.R. Marder, and J.W. Perry, Opt. Lett. **22**, 1843 (1997).
[14] B.A. Reinhardt, L.L. Brott, S.J. Clarson, A.G. Dillard, J.C. Bhatt, R. Kannan, L.X. Yuan, G.S. He, and P.N. Prasad, Chem. Mater. **10**, 1863 (1998).
[15] J.E. Rogers, B.C. Hall, D.C. Hufnagle, J.E. Slagle, A.P. Ault, D.G. McLean, P.A. Fleitz, and T.M. Cooper, J. Chem. Phys. **122**, 214708 (2005).
[16] H.S. Nalwa, Nonlinear Opt. Org. Mol. Polym., edited by H.S. Nalwa, S. Miyata (CRC Press, Boca Raton, 1997), p. 611.
[17] E. Badaeva, S. Tretiak, Chem. Phys. Lett. **450**, 322 (2008).
[18] X.J. Xing, J. Li, Y.P. Sun, and C.K. Wang, Theochem-J. Mol. Struct. **849**, 116 (2008).
[19] K. Ogawa, Y. Kobuke, J. Photochem. Photobiol., C **7**, 1 (2006).
[20] P. Lind, C. Lopes, K. Öberg, and B. Eliasson, Chem. Phys. Lett. **387**, 238 (2004).
[21] P. Lind, A. Eriksson, C. Lopes, and B. Eliasson, J. Phys. Org. Chem. **18**, 426 (2005).
[22] R. Vestberg, C. Nilsson, C. Lopes, P. Lind, B. Eliasson, and E. Malmström, J. Polym. Sci., Part A: Polym. Chem. **43**, 1177 (2005).
[23] J. Staromlynska, T.J. McKay, and P. Wilson, J. Appl. Phys. **88**, 1726 (2000).
[24] R. Vestberg, R. Westlund, A. Eriksson, C. Lopes, M. Carlsson, B. Eliasson, E. Glimsdal, M. Lindgren, and E. Malmström, Macromolecules **39**, 2238 (2006).
[25] Gaussian-03 Revision C.02, Frisch, M. J.; Trucks, G. W.; Schlegel, H. B.; Scuseria, G. E.; Robb, M. A.; Cheeseman, J. R.; Montgomery, Jr., J. A.; Vreven, T.; Kudin, K. N.; Burant, J. C.; Millam, J. M.; Iyengar, S. S.; Tomasi, J.; Barone, V.; Mennucci, B.; Cossi, M.; Scalmani, G.; Rega, N.; Petersson, G. A.; Nakatsuji, H.; Hada, M.; Ehara, M.; Toyota, K.; Fukuda, R.; Hasegawa, J.; Ishida, M.; Nakajima, T.; Honda, Y.; Kitao, O.; Nakai, H.; Klene, M.; Li, X.; Knox, J. E.; Hratchian, H. P.; Cross, J. B.; Bakken, V.; Adamo, C.; Jaramillo, J.; Gomperts, R.; Stratmann, R. E.; Yazyev, O.; Austin, A. J.; Cammi, R.; Pomelli,

C.; Ochterski, J. W.; Ayala, P. Y.; Morokuma, K.; Voth, G. A.; Salvador, P.; Dannenberg, J. J.; Zakrzewski, V. G.; Dapprich, S.; Daniels, A. D.; Strain, M. C.; Farkas, O.; Malick, D. K.; Rabuck, A. D.; Raghavachari, K.; Foresman, J. B.; Ortiz, J. V.; Cui, Q.; Baboul, A. G.; Clifford, S.; Cioslowski, J.; Stefanov, B. B.; Liu, G.; Liashenko, A.; Piskorz, P.; Komaromi, I.; Martin, R. L.; Fox, D. J.; Keith, T.; Al-Laham, M. A.; Peng, C. Y.; Nanayakkara, A.; Challacombe, M.; Gill, P. M. W.; Johnson, B.; Chen, W.; Wong, M. W.; Gonzalez, C.; and Pople, J. A.; . Gaussian, Inc., Wallingford CT, 2004.

[26] A.D. Becke, J. Chem. Phys. **98**, 5648 (1993).

[27] T.H. Dunning, J. Chem. Phys. **90**, 1007 (1989).

[28] A. Bergner, M. Dolg, W. Kuchle, H. Stoll, and H. Preuss, Mol. Phys. **80**, 1431 (1993).

[29] DALTON, a molecular electronic structure program, Release 2.0 (2005), see http://www.kjemi.uio.no/software/dalton/dalton.html.

[30] T. Yanai, D.P. Tew, and N.C. Handy, Chem. Phys. Lett. **393**, 51 (2004).

[31] M.J.G. Peach, T. Helgaker, P. Salek, T.W. Keal, O.B. Lutnaes, D.J. Tozer, and N.C. Handy, Phys. Chem. Chem. Phys. **8**, 558 (2006).

[32] W.J. Hehre, R. Ditchfield, and J.A. Pople, J. Chem. Phys. **56**, 2257 (1972).

[33] P. Norman, K. Ruud, Nonlinear optical properties of matter: From molecules to condensed phases, edited by M. Papadopoulos, J. Leszczynski, A.J. Sadlej (Kluwer Academic Press, 2006.

[34] M. Samoc, G.T. Dalton, J.A. Gladysz, Q. Zheng, Y. Velkov, H. Agren, P. Norman, and M.G. Humphrey, Inorg. Chem. **47**, 9946 (2008).

[35] D. Vincent, J. Cruickshank, Appl. Opt. **36**, 7794 (1997).

[36] D. Vincent, MCLC S&T, Section B: Nonlinear Optics **21**, 413 (1999).

[37] J.N. Demas, G.A. Crosby, J. Phys. Chem. **75**, 991 (1971).

[38] Jobin, Yvon, and Inc., "A Guide to Recording Fluorescence Quantum Yields", http://www.jobinyvon.com/usadivisions/fluorescence/applications/quantumyieldstrad.pdf.

[39] K. Sonogashira, Y. Tohda, and N. Hagihara, Tetrahedron Lett., 4467 (1975).

[40] M.A. Keegstra, A.J.A. Klomp, and L. Brandsma, Synth. Commun. **20**, 3371 (1990).

[41] T.S. Jung, J.H. Kim, E.K. Jang, D.H. Kim, Y.-B. Shim, B. Park, and S.C. Shin, J. Organomet. Chem. **599**, 232 (2000).

[42] S. Gronowitz, T. Frejd, Acta Chem. Scand., Ser. B **B30**, 313 (1976).

[43] S.J. Greaves, E.L. Flynn, E.L. Futcher, E. Wrede, D.P. Lydon, P.J. Low, S.R. Rutter, and A. Beeby, J. Phys. Chem. A **110**, 2114 (2006).

[44] J.S. Siddle, R.M. Ward, J.C. Collings, S.R. Rutter, L. Porres, L. Applegarth, A. Beeby, A.S. Batsanov, A.L. Thompson, J.A.K. Howard, A. Boucekkine, K. Costuas, J.F. Halet, and T.B. Marder, New J. Chem. **31**, 841 (2007).

[45] P. Norman, P. Cronstrand, and J. Ericsson, Chem. Phys. **285**, 207 (2002).

[46] J. Henriksson, P. Norman, and H.J.A. Jensen, J. Chem. Phys. **122**, 114106 (2005).

[47] J. Henriksson, U. Ekstrom, and P. Norman, J. Chem. Phys. **124**, 214311 (2006).

[48] D. Jacquemin, E.A. Perpete, G.E. Scuseria, I. Ciofini, and C. Adamo, J. Chem. Theory Comput. **4**, 123 (2008).

[49] M.J.G. Peach, P. Benfield, T. Helgaker, and D.J. Tozer, J. Chem. Phys. **128**, 044118 (2008).

[50] M.J. Paterson, O. Christiansen, F. Pawlowski, P. Jorgensen, C. Hattig, T. Helgaker, and P. Salek, J. Chem. Phys. **124**, 054322 (2006).

[51] T. Yasuda, T. Imase, Y. Nakamura, and T. Yamamoto, Macromolecules **38**, 4687 (2005).
[52] A. Baev, P. Norman, J. Henriksson, and H. Agren, J. Phys. Chem. B **110**, 20912 (2006).
[53] A. Baev, P. Welinder, R. Erlandsson, J. Henriksson, P. Norman, and H. Agren, Journal of Nonlinear Optical Physics & Materials **16**, 157 (2007).
[54] S. Dobrin, P. Kaszynski, and J. Waluk, J. Photochem. Photobiol., A **105**, 149 (1997).
[55] T.Y. Ohulchanskyy, D.J. Donnelly, M.R. Detty, and P.N. Prasad, J. Phys. Chem. B **108**, 8668 (2004).
[56] S.K. Chattopadhyay, B.B. Craig, J. Phys. Chem. **91**, 323 (1987).
[57] R. Hurley, A.C. Testa, J. Am. Chem. Soc. **90**, 1949 (1968).
[58] J. Lorenc, E. Kucharska, J. Hanuza, and H. Chojnacki, J. Mol. Struct. **707**, 47 (2004).

Figure captions:

Scheme. Pd-Cu-catalyzed cross-coupling in the synthesis of arylalkynyl-chalcogenophenes.

Figure 1. Compounds in the studied chalcogenophene series.

Figure 2. Theoretical two-photon absorption cross sections (σ^{TP}) for photon wavelengths in the visible region for eight chalcogenophenes (*upper and lower panels*). Results are obtained at the CAM-B3LYP/aug-cc-pVDZ level of theory.

Figure 3. Absorption spectra of chalcogenophenes **S1-Pe**, **S2-Pe**, **S3-Pe** and **Se1** (*upper panel*) and **O1-Pe**, **S1-OMe**, **S1-NO2-Pe** and **S1A-Pe** (*lower panel*), in THF.

Figure 4. Fluorescence emission from eight chalcogenophenes (*upper and lower panels*); ca. $2 \cdot 10^{-5}$ M in THF and 337 nm excitation wavelength. The emission traces of **Se1** and **S1-NO2-Pe** are enhanced by a factor of 10 for clarity.

Scheme:

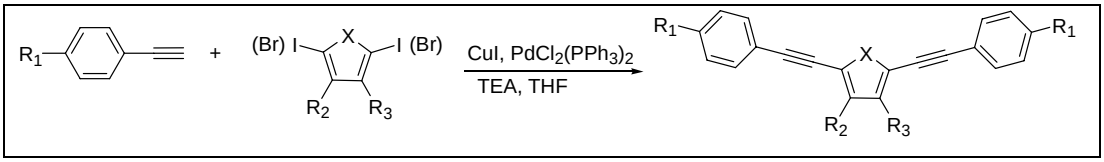

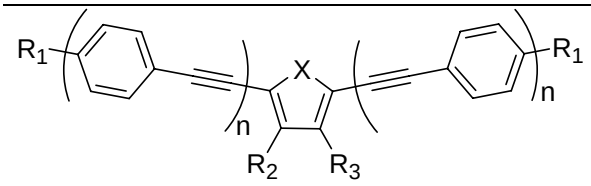

X = O, S, Se, Te
n = 1-3

Compound acronym	X	n	R_1	R_2	R_3
O1-Me	O	1	CH_3	H	H
S1, Se1, Te1	S, Se, Te	1	H	H	H
S2, Se2, Te2	S, Se, Te	2	H	H	H
S3, Se3, Te3	S, Se, Te	3	H	H	H
O1-Pe, S1-Pe	O, S	1	*n*-C_5H_{11}	H	H
S2-Pe, **S3-Pe**	S	2, 3	*n*-C_5H_{11}	*n*-$C_{12}H_{25}$	H
S1-OMe, **Se1-OMe**, **Te1-OMe**	S, Se, Te	1	OCH_3	H	H
S1-NO2a, **Se1- NO2a**, **Te1- NO2a**	S, Se, Te	1	NO_2	H	H
S1-NO2b	S	1	H	NO_2	NO_2
S1-NO2-Pe	S	1	*n*-C_5H_{11}	NO_2	NO_2
S1A-Pe	S	1	*n*-C_5H_{11}	CC-*p*-C_6H_4-*n*-C_5H_{11}	H

Figure 1.

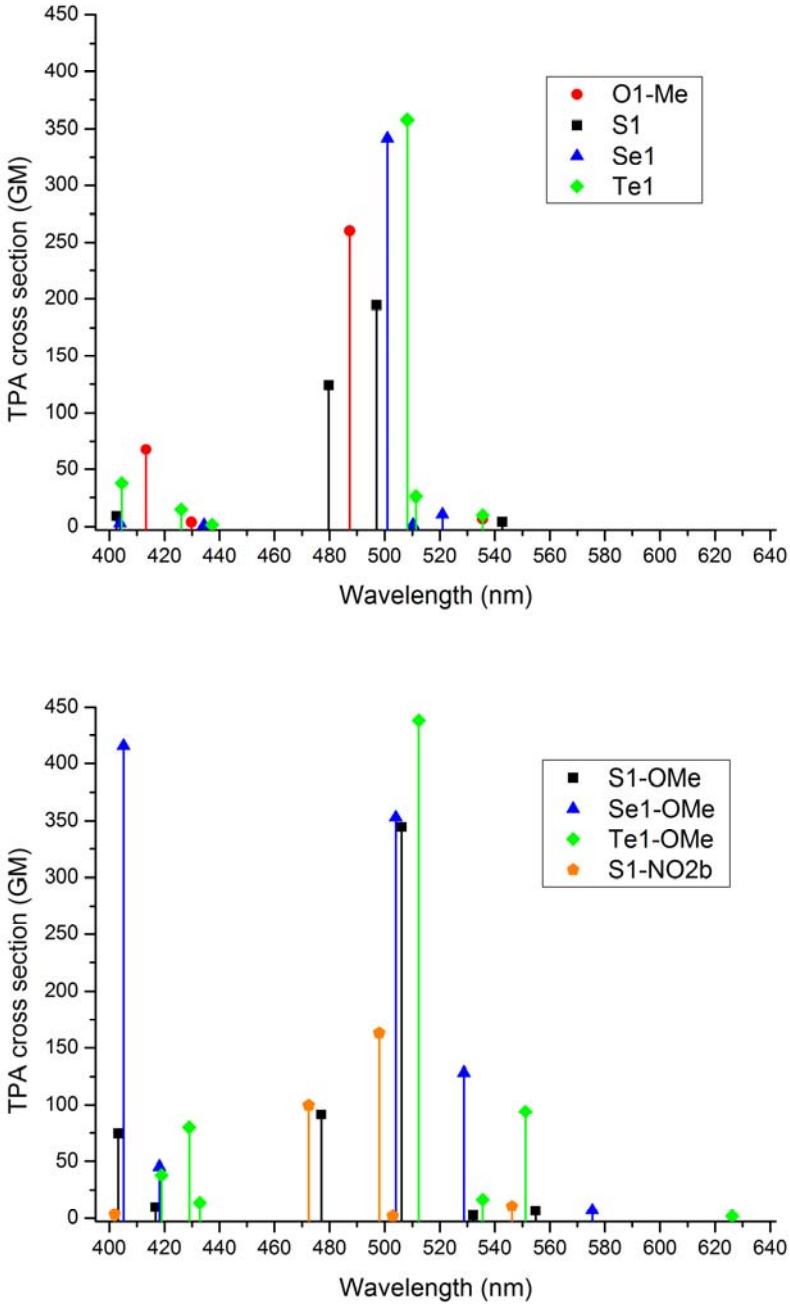
TPA cross section (GM)
Wavelength (nm)
O1-Me
S1
Se1
Te1
S1-OMe
Se1-OMe
Te1-OMe
S1-NO2b

Figure 2.

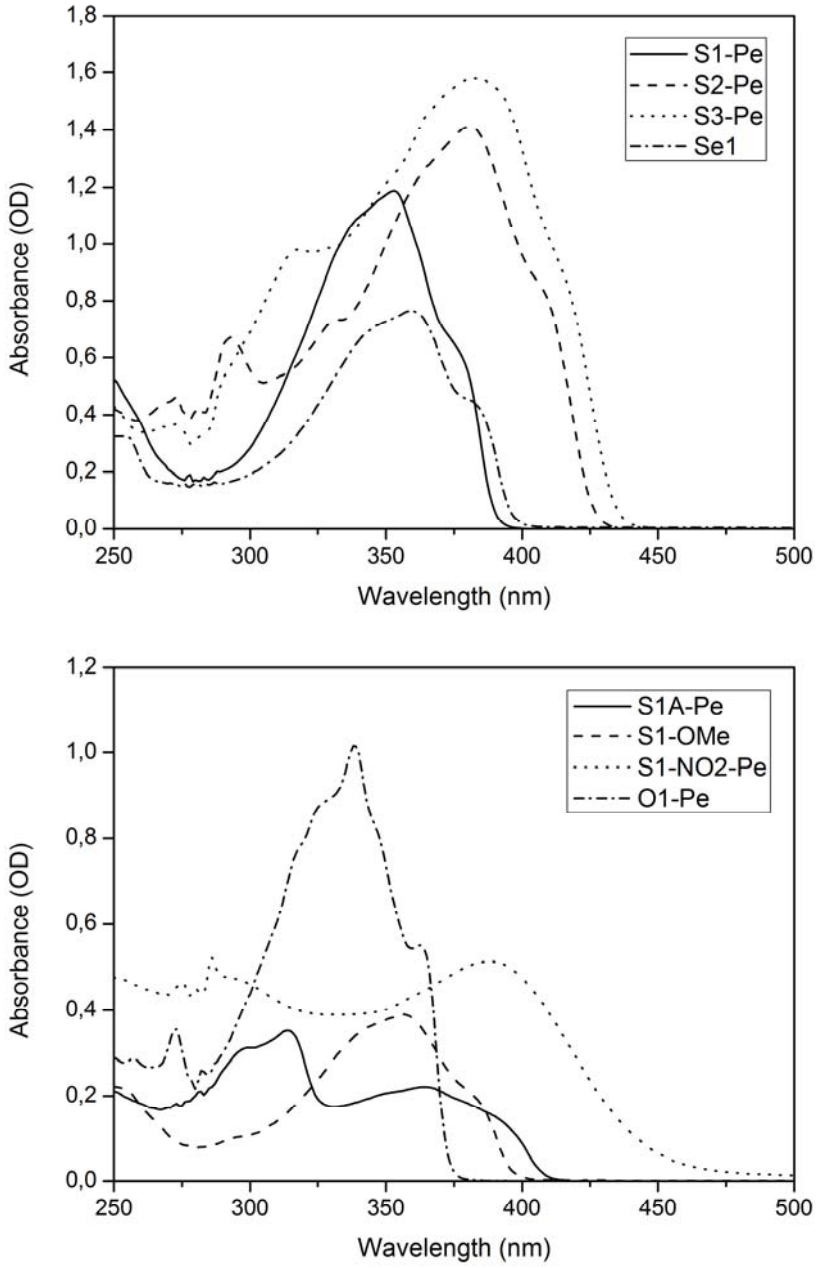
Absorbance (OD)
Wavelength (nm)
S1-Pe
S2-Pe
S3-Pe
Se1
S1A-Pe
S1-OMe
S1-NO2-Pe
O1-Pe

Figure 3.

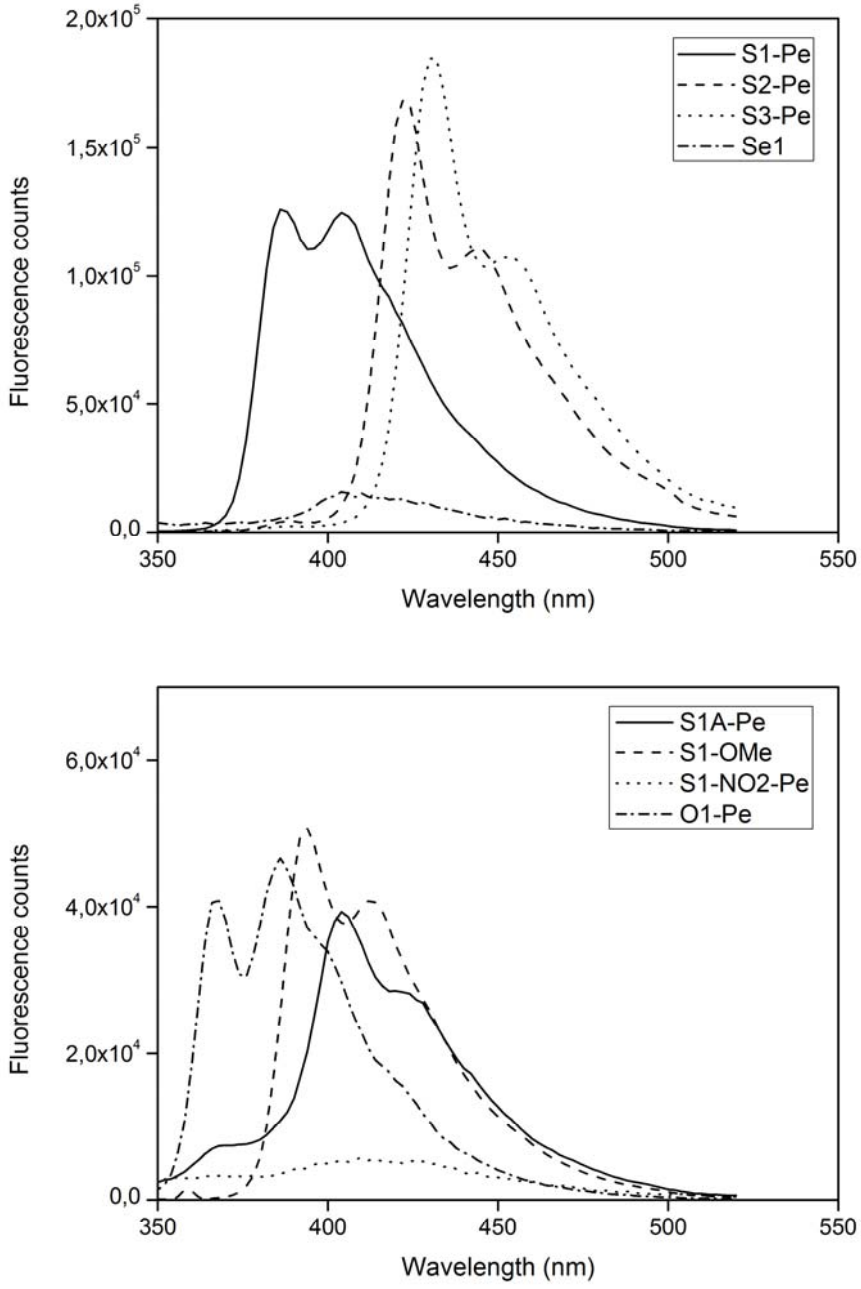
2,0x10^5
1,5x10^5
1,0x10^5
5,0x10^4
0,0
Fluorescence counts
350
400
450
500
550
Wavelength (nm)
S1-Pe
S2-Pe
S3-Pe
Se1
6,0x10^4
4,0x10^4
2,0x10^4
0,0
Fluorescence counts
350
400
450
500
550
Wavelength (nm)
S1A-Pe
S1-OMe
S1-NO2-Pe
O1-Pe

Figure 4.

Table 1. Calculated excitation wavelength (λ_{exc}) and oscillator strength (f) for the $X^1A_1 \rightarrow 1^1B_2$ transition for compound **S1**.

Basis set [a]	λ_{exc} (nm)			f		
	HF	B3LYP	CAM-B3LYP	HF	B3LYP	CAM-B3LYP
6-31G	327	382	345	1.35	1.57	1.56
6-31G, ECP	326	381	345	1.35	1.59	1.53
6-31++G, ECP(pd)	332	388	349	1.32	1.55	1.56
cc-pVDZ, ECP(pd)		395	358		1.56	1.53
cc-pVTZ, ECP(pd)	344	398	362	1.37	1.56	1.53
aug-cc-pVDZ, ECP(pd)			362			1.53
daug-cc-pVDZ, ECP(pd)			363			1.52

Note: [a] The parenthesis denotes the presence of polarization (p) and diffuse (d) functions in the ECP.

Table 2. HF and DFT calculated excitation wavelength and oscillator strength of the dominating singlet transition, $X^1A_1 \rightarrow 1^1B_2$, in chalcogenophene compounds.

Compound	HF/6-31G		B3LYP/6-31G		B3LYP/ cc-pVDZ		CAM-B3LYP/ aug-cc-pVDZ		Experimental [a]	
	λ_{exc} (nm)	f	λ_{exc} (nm)	f	λ_{exc} (nm)	f	λ_{exc} (nm)	f	λ_{max} (nm)	ε / 10^4 at λ_{max} (M^{-1} cm^{-1})
O1-Me	313	1.50	370	1.67	-	-	349	1.69	-	-
O1-Pe	-	-	-	-	-	-	-	-	338	5.1
S1	326	1.35	382	1.57	395	1.56	362	1.53	348	3.0
S1-Pe	-	-	-	-	-	-	-	-	352 [b]	3.5 [b]
S1-OMe [c]	329	1.54	395	1.82	407	1.81	368	1.77	356	3.3
S1-NO2a	-	-	-	-	447	1.70	389	2.60	-	-
S1-NO2b	298	1.11	385	1.44	-	-	360	1.46	-	-
S1-NO2-Pe	-	-	-	-	-	-	-	-	390	2.8
S1A-Pe	-	-	-	-	-	-	-	-	314, 358	4.2, 2.6
S2	-	-	449	3.06	467	3.08	-	-	-	-
S2-Pe	-	-	-	-	-	-	-	-	380 [b]	8.0 [b]
S3	-	-	479	4.32	-	-	-	-	-	-
S3-Pe	-	-	-	-	-	-	-	-	385 [b]	13 [b]
Se1	341	1.23	395	1.50	408	1.49	376	1.43	359	4.2
Se1-OMe	-	-	-	-	-	-	383	1.66	-	-
Se1-NO2a	-	-	-	-	-	-	407	2.05	-	-
Se2	381	2.38	462	3.02	480	3.04	-	-	-	-
Se3	-	-	491	4.26	512	4.32	-	-	-	-
Te1	353	1.15	407	1.44	420	1.43	389	1.36	-	-
Te1-OMe	-	-	-	-	-	-	396	1.58	-	-
Te2	404	2.10	473	2.98	491	3.00	-	-	-	-
Te3	-	-	500	4.21	522	4.28	-	-	-	-

Notes: [a] In THF. [b] Ref. [21]. [c] Two calculated stable conformers with different orientation of the OCH_3 groups have identical one-photon absorption properties.

Table 3. Dominating excited-state absorptions for $1^1B_2 \rightarrow n^1A_1$ transitions in the region of 400-850 nm. Results are obtained with use of the CAM-B3LYP functional and the aug-cc-pVDZ basis set (unless specified). Transitions with oscillation strength ≥ 0.02 are reported.

Compound	CAM-B3LYP/aug-cc-pVDZ	
	λ_{exc} (nm)	$f^{1\rightarrow n}$
O1-Me	807	1.021
	507	0.086
	461	0.084
S1	788	0.702
	709	0.377
	788 [a]	0.684 [a]
	711 [a]	0.378 [a]
	415 [a]	0.093 [a]
S1-OMe	806	1.033
	673	0.216
S1-NO2b	805	0.641
	684	0.302
Se1	842	0.04
	748	1.02
Te1	749	0.075
	735	0.946
Se1-OMe	737	0.861
Te1-OMe	825	0.042
	725	0.921

Note: [a] Calculated with the daug-cc-pVDZ basis.

Table 4. Optical power limiting and luminescence spectral data for chalcogenophenes in THF.

Compound	E_{out} (μJ) at E_{in} of 150 μJ, 532 nm [a]	λ_{fl} (nm) [b]	Stokes shift (nm) [c]	Q_{fl}	τ_{fl} (ns) [d]
O1-Pe	20 [e]	(368), 388	30	0.07	0.08
S1	25	383, (403) [f]	35	0.16 [f]	
S1-Pe	23 [e]	388, (405)	36	0.18	0.22
S1-OMe	18.5 [e]	394, (412)	38	0.17	0.24 (88 %) 0.06 (12 %)
S1-NO2-Pe	13 [g]	400-430 [h] 525-540 [f,h]	~10-40 [h] ~135-150 [f,h]	<0.001 [h] <0.004 [f,h]	6 (67 %) [h] 1 (22 %) [h] 0.1 (11 %) [h]
S1A-Pe	20	(368), 404, (422)	46	0.09	0.18 (95 %) 3.7 (5%)
S2-Pe	16 [i]	422, (444)	42	0.41	0.39
S3-Pe	14 [i]	431, (454)	46	0.50	0.42
Se1	20 [e]	400	41	<0.001 [h]	6 (13 %) [h] 1 (3 %) [h] 1-10 $\cdot 10^{-3}$ (84 %) [h,j]

Notes: [a] Conc. 0.010 M. [b] Conc. ≤ $2 \cdot 10^{-5}$ M. Excitation at 360 nm except for **S1-OMe** where this was 337 nm. Values in parenthesis are for smaller peaks or shoulders of the main peak(s). [c] Difference between the lowest-energy and highest-energy peak in the absorption and emission spectrum, respectively. [d] Percentage values in parenthesis are for decays which were best fitted with a two- or three-component exponential function. [e] Ref. [20]. [f] Measured in $CHCl_3$. [g] Measurements performed at a maximum of 120 μJ for E_{in}. E_{out} = 13 for E_{in} = 65-120 μJ. [h] Uncertain because of very weak emission. [i] Ref. [21]. [j] Uncertain because of instrumental limitations in the ps region.